

In-Vitro Cell Quantification Method Based on Depth Dependent Analysis of Brain Tissue Microscopic Images

Mustafa M. Sami, Yasuhisa Tamura, Cui Yilong, Hisakazu Kikuchi, and Yosky Kataoka

Abstract—In this study we developed a new automatic quantification method to count the number of targeted fluorescently labeled molecules of in-vitro rat brain tissue images. NG2+ glial cells were monitored in order to detect their proliferation to their same kind of cells or to another astrocyte cells using different fluorescently labeled molecules. The method is based on morphological segmentation followed by depth-dependent detection operation applied to a stack of confocal microscopic images. The number of local maxima peak points was used to count the number of the labeled cells. The method shows good promise for the computer-aided assessment in neurological studies for accurate automatic counting systems.

I. INTRODUCTION

Observing fluorescently labeled molecules in cells is a well-known technique to observe cellular changes, and hence it is applied in different biological studies. An important study shows that the continuous reproduction of neurons in adult mammals is found in two brain regions; the sub-ventricular zone (SVZ) of lateral ventricle and the sub-granular zone of the hippocampal dentate gyrus [1-2]. Therefore, the detection of cellular proliferating behavior in different brain regions is targeted by many researchers using different fluorescently labeled markers. These fluorescently labeled spots are usually counted manually through a visual inspection under the microscope or from captured images.

In our published paper [3], the counting procedure of the positively labeled molecules was achieved manually. The manual count is known to be slow, laborious, and subjective. In this work we intended to extend our study by developing a new computer-aided quantitative method using image processing and analysis techniques in order to count those fluorescently labeled molecules automatically. Our approach can be divided into several well-defined stages as illustrated in Fig.1.

After injecting the rats with 5-bromodeoxyuridine (BrdU), the brain is removed from the skull and processed using the

standard neurological procedure. Serial sections were cut to a thickness of 30 μ m using a microtome and then captured using a high resolution camera. After image acquisition, the fluorescently labeled molecules are segmented based on the color information applied to each color-channel in the RGB color space. After segmentation, a morphological filter is applied so as to remove artifacts which are not topologically part of the segmented objects. Next, a median filter is applied to the previously separated RGB channels as a pre-processing step to reduce the noise before measuring the depth signal. A depth-dependent detection operation is used in order to generate a signal from the central points of the objects in those noise filtered images. Finally, the count of the labeled cells is computed automatically based on the number of local maxima peak points of the generated signals.

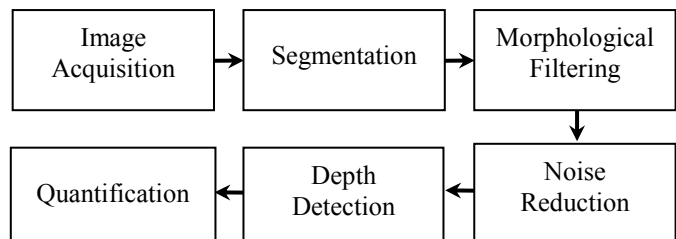


Fig. 1. Schematic structure of the computer-aided method.

The details of the method are described in the following sections. Section 2 will give some basic information about the neurological background of this study, while Section 3 and Section 4 will describe the materials and methods respectively. Section 5 provides some experimental results using real samples. Finally, some concluding remarks are given in Section 6.

II. NEUROLOGICAL BACKGROUND OF THE STUDY

This section introduces some basic concepts related to cell proliferation in the brain tissue. However, it is not the aim to explore it here in details that could be found in our paper [3]. The paper is focused on the doublecortin- and NG2-immunopositive progenitor cells in the adult rat neocortex.

In general, the brain cells in adult mammals can be categorized into three main groups: neurons, glial, and blood vessel cells. We are interested in the glial cells which are divided into two subgroups of cells: 1) proliferative glial cells (include microglia and NG2+ cells) and 2) non-proliferative glial cells. The core of the study is to identify the NG2+ differentiation using different fluorescently

Manuscript received April 13, 2011.

M.M. Sami author is with Cellular Function Imaging Laboratory, RIKEN Center for Molecular Imaging Science, Kobe, and also with Department of Electrical and Electronics Engineering, Graduate School of Science and Technology, Niigata University, JAPAN (email: mustafa@riken.jp).

Y. Tamura, C. Yilong, and Y. Kataoka authors are with Cellular Function Imaging Laboratory, RIKEN Center for Molecular Imaging Science, Kobe, JAPAN (email: tamuray@riken.jp, cuiyl@riken.jp, kataokay@riken.jp).

H. Kikuchi author is with Department of Electrical and Electronics Engineering, Niigata University, JAPAN (email: kikuchi@eng.niigata-u.ac.jp).

labeled markers that appear green, blue, and red color under the confocal microscope. NG2+ cells can be traced by using BrdU as a marker for the proliferation activity of glial cells and fluorescently appears as a green labeled area as shown in Fig. 2. The result from this proliferation activity is either a daughter cells of the same kind of NG2+ cells which is fluorescently labeled as a red colored area using OLIG2 biomarker, or to another kind of astrocyte cells that appear blue colored area using GFAP biomarker. Therefore, our automated counting method is to calculate the number of these green labeled cells, and also their intersection with the red and blue cells that represent the proliferation activity.

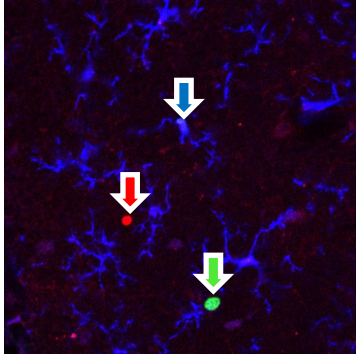


Fig. 2. The green arrow indicates BrdU fluorescently labeled area of NG2+ immunopositive proliferative glial cells. While the blue and red arrows indicate the OLIG2 and GFAP immunopositive cells respectively.

III. MATERIALS

A. Animals and BrdU Injection

Adult male Wister rats were used in our investigation. All experimental protocols were approved by the Ethics Committee on Animal Care and Use. For labeling of proliferating cells, adult rats ($n = 15$) were intraperitoneally injected with BrdU at 50 mg/kg body weight. Each animal underwent a single injection of BrdU.

B. Immunohistochemistry

Animals were deeply anesthetized with diethyl ether and perfused transcardially with 4% formaldehyde buffered with 0.1 M phosphate buffered saline at 2 h, 14 days and 28 days after injection of BrdU. Brains were removed, postfixed overnight at 4 °C in 4% formaldehyde buffered with 0.1 M PBS and then immersed in 20% (w/v) sucrose solution. Coronal brain sections (30 μ m thickness) were prepared using a cryostat and collected as free-floating sections. For detection of BrdU incorporation, brain sections were preincubated in 50% formamide/2, standard sodium citrate (SSC) for 2 h at 65 °C, incubated in 2 N HCl for 30 min at 37 °C, rinsed in 0.1 M boric acid (pH 8.5) for 10 min at 25 °C, and then washed with 0.3% Triton X-100 in PBS (PBST). For multiplex-immunostaining, coronal sections were incubated with several antibodies for 12–36 h at 4 °C [3].

IV. AUTOMATIC COUNTING METHOD

A. Acquisition

The tissue samples were acquired under the same magnification of 20 \times and with 848 \times 832 pixel resolution using a confocal laser microscope (LSM510META Ver. 3.2; Carl Zeiss). A stack of 20 digital images was generated from each sample and saved in TIFF format and delivered to the engineering authors for further investigations.

B. Segmentation

As mentioned in Sec. 2, the captured images contain three different fluorescently labeled markers and indicated as green, blue, and red areas in the captured images as shown in Fig. 2. The objective from this computer-aided system is to be able to count; **1**) the nuclei of NG2+ cells (green area); **2**) the proliferated NG2+ cells that produced a daughter NG2+ cells (green area intersect with red area); **3**) the proliferated NG2+ cells that produced another kind of astrocyte cells (green area intersect with blue area).

Since the three targeted spots are with three different colors, the labeled nuclei are separated based on their color information. Thus, the RGB color space is assumed to work sufficiently to separate these labeled areas. The green G-channel is used to segment the NG2+ cells, and similarly the red R-channel is used to segment the daughter NG2+ cells, while the blue B-channel is used to segment the astrocyte cells. It is important to note that the intersection between the G-channel and R-channel will indicate the proliferated NG2+ cells to daughter cells of NG2+, while the intersection between the G-channel and B-channel will indicate the proliferated NG2+ cells to astrocyte cells. The whole process of the method is illustrated in Fig. 3.

At first, the observed cell's nuclei in the green channel are segmented by applying a global thresholding using the Otsu method [4] for binarization. This generates a bilevel image based on the intensity values of the green channels. Pixels with intensity values falling within a given range are determined as foreground (ones), while all other remaining pixels are determined as background (zeros). This binarization process will be applied to the whole stack consist of 20 G-channel frames separately. After that, these bilevel images will be summed together and this will generate a single binary image that includes the whole nuclei including the overlapped ones as well. Note that all nuclei falling within the same field of view will be observed as a single nucleus in this bilevel image as shown in Fig. 4. Therefore, to identify these overlapping nuclei we developed a depth-dependent detection operation and it will be described later in this section.

Next, a morphological filter is applied to the bilevel image so as to remove the undesired artifact pixels which are not topologically part of the targeted features. Thus, objects in the obtained bilevel image are thickened by adding pixels to the exterior of the objects until doing so would result in previously unconnected objects being 8-connected. Note that a pixel is said to be 8-connected, if it is connected to at least one of 8 immediate neighbors. The resultant image from this

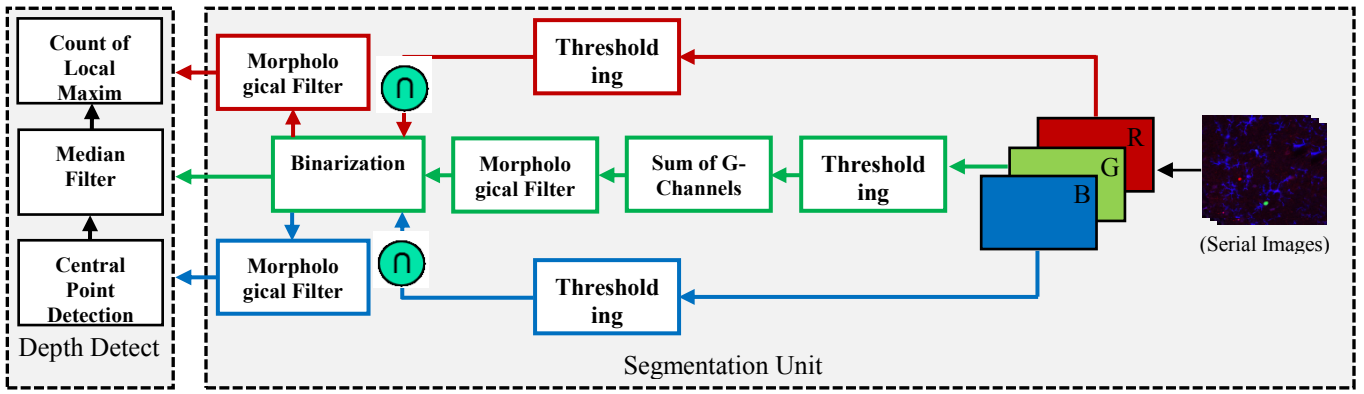


Fig. 3. The sequence of the different operations used by the computer-aided counting system.

thickening is referred to as I . Separately, the same binary image objects will be bridged in order to connect the objects separated by a single pixel gaps, and we will call this image J . Both the thickened and the bridged images are added together $I+J$ and this will assure us that the closest objects near to the nuclei are joined into the nuclei and only those objects relatively far away are discarded [6-7].

The above mentioned thickening [5] of a bilevel image A is defined as

$$A \odot B = A \cup (A * B) \quad (1)$$

where \cup denotes the union of two sets. B is a pair of structuring elements, $B = (B_1, B_2)$, used in the hit-or-miss transformation [18] in such a way that

$$A * B = (A \ominus B_1) \cap (A^c \ominus B_2) \quad (2)$$

where \cap stands for the intersection of two sets. $A \ominus B_1$ indicates the erosion of A by B_1 and A^c is the background.

A morphological opening operation using a 6×6 square structuring element is applied to the image, $I+J$. Morphological opening is the erosion of A by B followed by dilation by B . The erosion of A by B is defined as

$$A \ominus B = \{z \mid (B)_z \cap A^c \neq \phi\} \quad (3)$$

where $(B)_z$ denotes the structuring element B translated by z and ϕ is the empty set. The dilation of A by B is expressed by

$$A \oplus B = \{z \mid (\hat{B})_z \cap A \neq \phi\} \quad (4)$$

where $(\hat{B})_z$ stands for the translation of B by z of the reflection about the origin. The image is then to be closed by a morphological closing operation (dilation followed by erosion) using the same 6×6 square structuring element.

To this end, the segmented feature represents the NG2+ cells (Fig. 4 (a)), and by finding its intersection with the similarly segmented feature from the blue and red channels

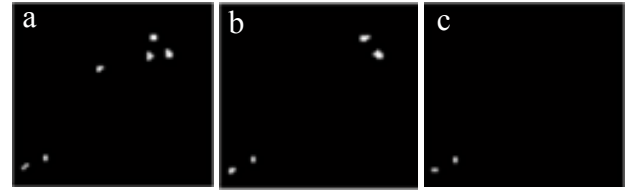


Fig. 4. Segmented fluorescently labeled areas. (a) NG2+. (b-c) NG2+ intersects with GFAP and OLIG2 respectively.

this will generate an image that represents the proliferated cells as shown in Fig. 4 (b) and (c).

C. Depth-Dependent Detection

The number of the segmented cells in Fig. 4 does not always represent the actual number of the targeted cells. This is because it is possible that two or more cells are overlapped or located within the same field of view as illustrated in Fig. 5. Such a problem is common in confocal microscope imaging since the stacked images represent a whole volume but observed from one field of view. Therefore, we developed a depth-dependent detection method for this purpose. The method is based on the assumption that in confocal laser imaging the intensity of an object starts with low values then increases gradually until it reach to a maximum intensity value before it starts to decrease and reach again to a low intensity values as illustrated in Fig. 5. If we imagine a line that pass through the center of the summed stack images in Fig.4 but it goes through the whole 20 frames of the green G-channels, this line will have 20 intensity values. By plotting these intensity values, the number of peaks of local maxima will represent the actual number of cells.

The x-y coordinates of a central point of an object is defined as vector that specifies the center of mass of the region. As a pre-specifies step, we applied a small size mean filter of size 3×3 to all green G-channel stack images in order to reduce the noise by obtaining an averaged intensity value of the central points. Finally, the number of peak-points in the generated plots of these central-points is computed, where the number of local maxima peak points represents the number of objects as shown in Fig. 6.

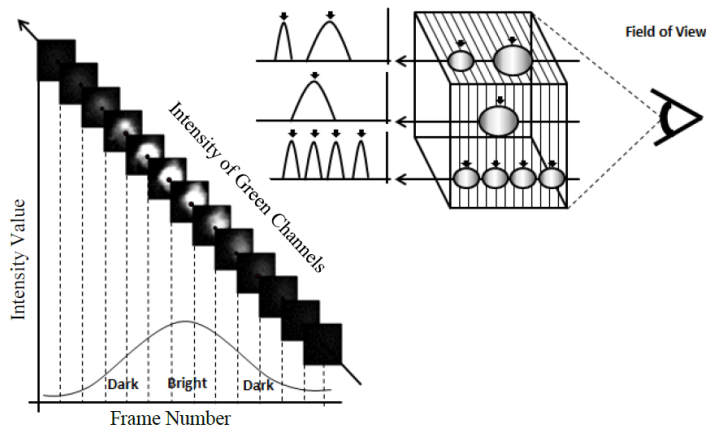


Fig. 5. Different depth intensities of the green channel of a segmented cell generated from a confocal laser microscope.

V. EXPERIMENTAL RESULTS USING REAL SAMPLES

Table I shows part of the results for 5 tested samples. The table shows the count for the NG2+ cells (green), NG2+ that changed to an astrocyte cells (green-blue), and NG2+ that proliferated to a daughter cell of NG2+ (green-red). The table provides a comparison between the manual and automatic count using the developed computer-aided system.

The plots in Fig. 6 show the detected depth-dependent signal that has been used in this study for the 7 segmented cells shown in Fig.4. Each plot represents the intensity values over the 20 G-channels passing through the center of the cells. Among the observed 7 cells, 6 of them have only a single peak point which indicates that these 6 cells are without overlapping. But one cell shows two peak points which indicates that it has two overlapped cells. Therefore, the actual total number of cells in Fig. 4 is 8 cells although only 7 cells appear at the segmented image. This count was confirmed by applying an intensive manual check for the sample which was very hard to be detected by our eyes using the usual manual count.

TABLE I
COMPARISON BETWEEN AUTOMATIC AND MANUAL COUNT

Sample		Automatic Count	Manual Count
Sample 1	Green	12	12
	Green-Blue	12	10
	Green-Red	11	11
Sample 2	Green	15	14
	Green-Blue	15	11
	Green-Red	14	10
Sample 3	Green	8	8
	Green-Blue	7	5
	Green-Red	7	5
Sample 4	Green	9	9
	Green-Blue	4	4
	Green-Red	2	0
Sample 5	Green	3	3
	Green-Blue	1	1
	Green-Red	0	0

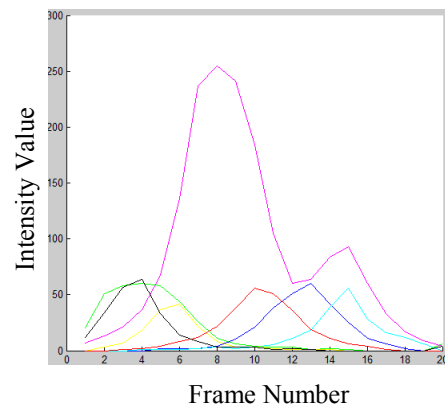


Fig. 6. Depth intensities of a real sample. The graph includes 6 plots with a single local maxima and one plot has two local maxima peaks.

We have developed the software package with the name *Eguchi Cell Count* that implements the counting system described in this paper. A user friendly front-end graphical user interface (GUI) has been designed to aid biologists to count the desired fluorescently labeled molecules automatically.

VI. CONCLUSION

A new computer-aided quantification method has been developed to automatically count the fluorescently labeled cells appears in a stack images generated by a confocal laser microscope. The method was able to detect precisely the overlapped cells which were very hard to be observed by human eyes. The method shows a good promise for the automatic counting systems used in neurological studies.

REFERENCES

- [1] H. A. Cameron et al., "Differentiation of newly born neurons and glia in the dentate gyrus of the adult rat", *Neuroscience*, vol. 56, pp. 337-344, 1993.
- [2] C. Lois et al., "Proliferating subventricular zone cells in the adult mammalian forebrain can differentiate into neurons and glia", *Proc. Natl Acad. Sci. USA*, vol. 90, pp. 2074-2077, 1993.
- [3] Y. Tamura et al., "Multi-directional differentiation of doublecortin- and NG2-immunopositive progenitor cells in the adult rat neocortex in vivo", *European Journal of Neuroscience*, vol. 25, pp. 3489-3498, 2007.
- [4] N. Otsu, "A threshold selection method from gray-level histograms," *IEEE Trans. Systems, Man, and Cybernetics*, vol. SMC-9, no. 1, pp.62-66, Jan. 1979.
- [5] R. C. Gonzalez and R. E. Woods, *Digital Image Processing*, 2nd ed., Prentice Hall, 2002.
- [6] M. Sami et al., "A computer-aided distinction of borderline grades of oral cancer," *IEEE ICIP 2009*, pp. 4205-4208, Cairo, Nov. 2009.
- [7] M. Sami et al., "Shape Analysis of the Rete Processes for Borderline Malignancies of the Oral Mucosal Epithelia," *Proc. EMBBE 2008*, CD ROM, Porto, Mar. 2008.